

https://doi.org/10.1070/QEL16238

Combined optical parametric oscillator with continuous tuning of radiation wavelength in the spectral range 2.5–10.8 μm

D.B. Kolker, I.V. Sherstov, N.Yu. Kostyukova, A.A. Boyko, K.G. Zenov, R.V. Pustovalova

Abstract. **A combined optical parametric oscillator (OPO) with continuous tuning of the radiation wavelength in the spectral range 2.5–10.8 μm, optically pumped with the radiation from a *Q*-switched Nd:YLF laser (1.053 μm), is developed and tested. The oscillation is provided by an OPO1 based on a MgO:PPLN 'fan-out' structure in the spectral region 2.5–4.5 μm and by an OPO2 based on $HgGa_2S_4$ nonlinear crystals in the spectral region 4.18–10.8 μm, respectively. The angles of phase matching are measured for the $HgGa_2S_4$ crystals in the spectral range 4.18–10.8 μm for the type II conversion (eo-e), which virtually coincide with the calculated ones. The experimental absorption spectra of a gas mixture in the range 2.5–10.8 μm obtained using a gas-filled sealed-off photoacoustic cell are presented.**

Keywords: *optical parametric oscillator, MgO:PPLN 'fan-out' structure, $HgGa_2S_4$ nonlinear crystal.*

1. Introduction

To date, one of the urgent problems in the environmental studies is the remote and local analysis of the atmosphere gas composition using lasers [1], including the methods of laser photoacoustic spectroscopy [2–6], etc. [7]. One of the advantages of the laser gas analysis is that the information is collected almost in real time. The most informative range for performing such atmospheric analysis is the mid-IR range (2–14 μm), since it covers the basic vibration–rotation absorption bands of various molecules [8], interesting for researchers. However, the absence of mid-IR lasers, tunable in a wide range of wavelengths, hampers the development of these studies. The problem can be solved using optical parametric oscillators (OPOs) [9]. A number of papers devoted to the laser gas analysis of atmosphere using OPOs [10, 11] confirm the urgency of this line of research. At present different types of OPOs are fabricated that can provide continuous tuning of the radiation wavelength in particular segments of the spectral range 2–12 μm [12–20].

In the spectral region 2.5–4.5 μm, the most efficient nonlinear media for OPOs are periodically polarised structures of lithium niobate doped with magnesium (MgO:PPLN). Lithium niobate crystals are transparent in the spectral range 0.3–4.5 μm. To pump MgO:PPLN structures, use is commonly made of lasers with the radiation wavelength 1.053–1.064 μm. At wavelengths exceeding 4.5 μm, the parametric oscillation in such structures is low-efficient due to the absorption in lithium niobate. At present, MgO:PPLN structures are implemented in different versions, namely, with a constant period, with a varied period ('fan-out' configuration), and as aperiodic structures [12–15].

For OPOs in the spectral range 4–12 μm, use is made of different nonlinear optical crystals of the mid-IR range ($AgGaS_2$, $AgGaSe_2$, $ZnGeP_2$, $LiInSe_2$, $HgGa_2S_4$, $BaGa_4S_7$, etc.) [9, 16–20]. For the present work, based on the combination of the parameters, we have chosen for the OPO with the tuning range 4–11 μm a nonlinear crystal $HgGa_2S_4$ (below referred to as HGS) produced at the Kuban State University (Krasnodar, Russia) [21]. The HGS crystals are transparent in the spectral range 0.55–13 μm, which allows their pumping with the radiation of lasers having the wavelength 1.053–1.064 μm. According to the literature data known at the time of the study, only two separate intervals 3.7–5.7 μm [18] and 4.5–9 μm [19] are covered by HGS OPOs.

The present work is devoted to the development and investigation of a combined OPO with continuous tuning of the radiation wavelength in the spectral range 2.5–10.8 μm aimed at using in a laser photoacoustic gas analyser.

2. Experimental setup

To provide continuous tuning of the radiation wavelength in a wide spectral range, we developed an optical scheme of a combined OPO presented in Fig. 1. The scheme incorporates two different OPOs, one of them being based on a 'fan-out' MgO:PPLN structure and the other – on nonlinear HGS crystals, tunable within different spectral ranges and pumped with the radiation of a single Nd:YLF laser (1.053 μm).

The experimental setup incorporates a pump Nd:YLF laser, an optical Faraday isolator, a half-wave plate, different mirrors and lenses, optical cavities of the optical parametric

D.B. Kolker, I.V. Sherstov Institute of Laser Physics, Siberian Branch, Russian Academy of Sciences, prosp. Akad. Lavrent'eva 13/3, 630090 Novosibirsk, Russia; Novosibirsk State University, ul. Pirogova 2, 630090 Novosibirsk, Russia; e-mail: kolker@ngs.ru, sherstov@ngs.ru;
N.Yu. Kostyukova, A.A. Boyko Novosibirsk State University, ul. Pirogova 2, 630090 Novosibirsk, Russia; Special Technologies Ltd., ul. Zelenaya gorka 1/3, 630090 Novosibirsk, Russia; e-mail: n.duhovnikova@gmail.com;
K.G. Zenov Special Technologies Ltd., ul. Zelenaya gorka 1/3, 630090 Novosibirsk, Russia; e-mail: zkg@ngs.ru;
R.V. Pustovalova Institute of Laser Physics, Siberian Branch, Russian Academy of Sciences, prosp. Akad. Lavrent'eva 13/3, 630090 Novosibirsk, Russia; e-mail: pustovalova_r@mail.ru

Received 18 October 2016; revision received 27 October 2016
Kvantovaya Elektronika **47** (1) 14–19 (2017)
Translated by V.L. Derbov

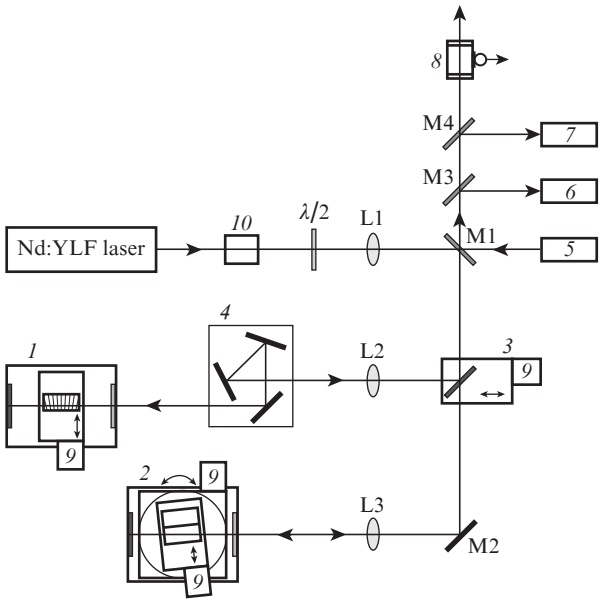

Figure 1. Optical block scheme of the experimental setup: (*1*) optical parametric oscillator OPO1; (*2*) optical parametric oscillator OPO2; (*3*) channel selector; (*4*) angle reflector; (*5*) alignment laser; (*6*) wavelength meter; (*7*) power meter; (*8*) gas-filled PA cell; (*9*) stepper motors; (*10*) Faraday optical isolator; ($\lambda/2$) half-wave plate; (L1–L3) lenses; (M1–M4) mirrors.

oscillators OPO1 and OPO2, a channel selector, a angle reflector, an alignment laser, power and wavelength meters, and a photoacoustic (PA) gas-filled cell. In the spectral range 2.5–4.5 μm, the oscillation is provided by the OPO1 based on the 'fan-out' MgO:PPLN structure, and in the spectral region 4.18–10.8 μm the oscillation is provided by the OPO2 based on the nonlinear HGS crystals.

A combined PPLN and HGS OPO was pumped by a *Q*-switched Nd:YLF laser (Laser compact, model TECH-1053-N) at 1.053 μm (TEM_{00}) with horizontal polarisation. The pulse energy achieved 1.3 mJ, the duration was ~16 ns, the repetition rate was set within the interval from 200 to 2000 Hz.

By means of mirrors, the radiation beam from the pump laser was directed to the optical cavity of OPO1 or OPO2, where the parametric conversion of the radiation wavelength occurred. The channel selector, switching the direction of the pump beam propagation to OPO1 or OPO2, is a flat reflecting mirror mounted on a linear stepper motor stage. The angle reflector, installed in front of OPO1, serves to rotate the radiation polarisation plane by 90°. It is comprised by three flat reflectors with silver coating that reflect the incident beam according to the 'rightwards (90°) – downwards (90°) – forwards (90°)' scheme.

The mid-IR output radiation from OPO1 or OPO2 passes through the dichroic mirror M1. Then, the measurement of the pulse energy and the radiation wavelength is performed. The pulse energy is measured using a PE10-C meter (Ophir Vega). The wavelengths of radiation from OPO1 and OPO2 are determined using Angstrom LSA IR (0.8–1.75 μm) and WS/6 IR-III (2–11 μm) meters. The auxiliary gas-filled cell is used to control the operating radiation wavelength of OPO1 or OPO2 by using for reference the characteristic absorption peaks of the gas admixtures filling it.

3. Experimental results

3.1. Testing OPO1

In the present work we used the 'fan-out' MgO:PPLN structure, installed in the OPO1 cavity, having the dimensions 45 × 25 × 1 mm and the period smoothly varying in the range 27.5–32.5 μm. The structure faces were AR coated and had a transmission coefficient maximum at λ = 1.5 μm. The flat input/output coupler and the total reflector formed the OPO1 50 mm long cavity. The input/output coupler was transparent for the pump laser radiation (T = 98% at λ = 1.053 μm) and for the idler wave ($T \approx 95\%$ at λ = 2.5–4.5 μm), while for the signal wave (1.35–1.7 μm) the reflection coefficient of the output coupler amounted to ~99%. The reflector had a silver coating.

To move the structure inside the OPO1 cavity, we used a linear stepper motor stage (the total move is 25 mm and the resolution is 1.25 μm per step), on which the 'fan-out' MgO:PPLN structure enclosed in a thermostat was installed. The thermostat kept the temperature constant at a level of 40 ± 0.1 °C. The smooth tuning of the OPO1 radiation wavelength was implemented by means of the precision horizontal translation of the 'fan-out' MgO:PPLN structure perpendicular to the cavity axis.

The pulse energy of the Nd:YLF pump laser was 0.8 mJ, the repetition rate was 1000 Hz. The radiation of the pump

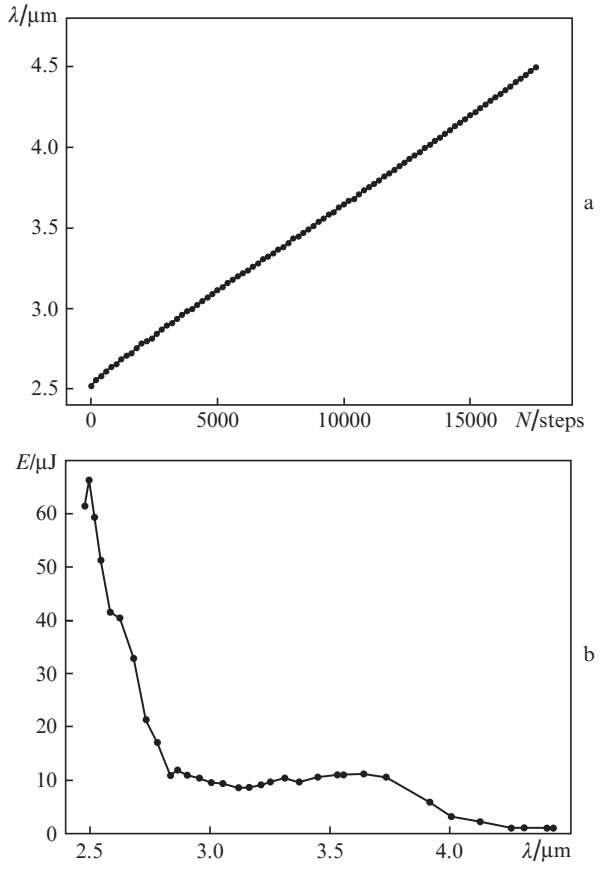

Figure 2. (a) Tuning characteristic of the OPO1 idler wave as a function of the position of the motorised linear stage and (b) dependence of OPO1 radiation pulse energy on the wavelength.

laser was focused so that the diameter of the beam in the centre of the structure amounted to ~0.5 mm, the energy density being ~0.4 J cm^{-2}. The pump radiation and the radiation output from OPO1 had vertical polarisation that changed for horizontal one after passing the angle reflector (*4*) (see Fig. 1).

Figure 2a presents the tuning characteristic of OPO1 depending on the position of the motorised linear stage. In the experiment, we obtained smooth continuous scanning of the idlerr radiation wavelength from OPO1 in the spectral range 2.5–4.5 μm, which corresponds to the frequency interval ~1777 cm^{-1}. The OPO1 tuning characteristic is practically linear in this range with the slope ~0.11 nm step^{-1} (~0.12 cm^{-1} step^{-1} at the wavelength of 3 μm). In the present work no special measures were undertaken to reduce the OPO1 radiation spectral width, e.g., we used neither an intracavity etalon [11], nor a diffraction grating [10]. The spectral width of the OPO1 oscillation was determined indirectly, when recording the absorption spectra of different gas components [22], and was estimated to be no smaller than ~5 cm^{-1}.

The studies of the energy parameters of the OPO1 radiation were carried out. Figure 2b presents the dependence of the OPO1 idlerr wave radiation pulses energy on the wavelength in the spectral range 2.5–4.5 μm. The greatest pulse energy (~67 μJ) was observed at λ = 2.5 μm, after which it monotonously decreased with increasing wavelength. In the spectral interval 3.4–3.7 μm the pulse energy amounted to ~10 μJ. In the range of wavelengths exceeding 4.0 μm the pulse energy of the idler wave sharply decreased due to the increasing absorption in the nonlinear element itself. At the wavelength near 4.3 μm the influence of absorption by the atmospheric CO_2 on the pulse energy was detected.

Kolker et al. [15] report the results of OPO1 tests using two similar 'fan-out' MgO:PPLN structures. Continuous tuning of the idler wavelength within the spectral ranges 2.4–3.1 and 3.3–3.85 μm was obtained.

3.2. Testing OPO2

Tyazhev et al. [23] showed that the maximum efficiency of parametric frequency conversion in HGS crystals for the idler wavelength exceeding 5 μm is achieved using type II interaction and crystals cut at the angle φ = 0. Figure 3 presents the calculated tuning curve for the idler wave of the OPO based on the HGS nonlinear crystal (type II conversion, eo-e), plotted using the improved-accuracy data from Ref. [24]. It is seen that the HGS crystal can provide continuous tuning of the OPO idler wave within the spectral range 3.5–12 μm by varying the angle θ in the crystal from 80 to 42°. In fact, it means that the crystal should be rotated by the angle no smaller than ± 45°, which is related to certain difficulties in practical implementation.

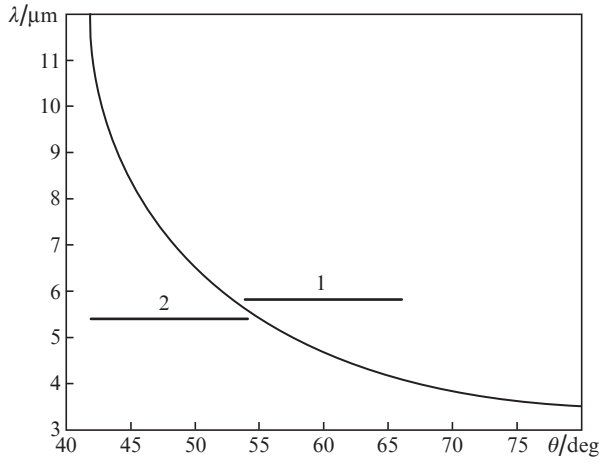

Figure 3. Calculated tuning characteristic of the OPO based on the HGS nonlinear crystal (type II, eo-e); segments 1 and 2 are the ranges of angular displacement of the HGS1 and HGS2 crystals, cut for different angles θ (see text).

In the present work in order to offer a wide tuning range, it is proposed to place two nonlinear HGS crystals in the OPO2 cavity instead of one crystal, as usually done (see Fig. 1). The crystals are cut at different angles for the eo-e interaction type. Such a layout of OPO2 allows essential reduction of the angular displacement of each crystal. The crystal HGS1 is cut so that the angles are θ = 60°, φ = 0 (for the idler wavelength ~4.7 μm at normal incidence). The crystal HGS2 is cut so that the angles are θ = 47°, φ = 0 (for the idler wavelength ~7.45 μm at normal incidence). Both crystals consist of the orange phase of HGS [21], possess similar sizes (13 × 5 × 5 mm) and are processed together. The faces of both crystals are AR coated and have the centre of the transmission spectrum at λ = 1.2 μm. The ranges of angular motion of both HGS crystals, implemented in the present work, are shown in Fig. 3 by segments of straight lines.

The dichroic input/output coupler and the total reflector formed the OPO2 23 mm long cavity. The dichroic input/output coupler with the curvature radius 1 m was transparent for the pump radiation ($T \approx 92\%$ at λ = 1.053 μm) and the idler wave of OPO2 ($T \approx 80\%$ at λ = 4.2–10.8 μm), while for the signal wave (λ = 1.17–1.4 μm) the transmission coefficient amounted to 5%–15%. The flat reflector had a silver coating.

Inside the OPO2 cavity two HGS crystals enclosed in a thermostat were installed, their temperature kept at a level of 25 ± 0.1 °C. The rotation of the nonlinear crystals in the *YZ* plane by the angle θ was performed within the range ±17° from the middle (normal for crystals) position with the step 0.005° by means of a rotary stepper motor stage. On the rotary stage, an auxiliary motorised linear stage was mounted to provide transverse displacements of the HGS crystals and sequential installation of one of the crystals into the operating position at the axis of the cavity (see Fig. 1).

The pump pulse energy from the Nd:YLF laser was 0.9 mJ, and the pulse repetition rate was 1000 Hz. The radiation beam of the pump laser at the input of the OPO2 cavity had the diameter ~0.5 mm and the energy density ~0.46 J cm^{-2}. The pump radiation and the idler wave of OPO2 were horizontally polarised. Preliminary results of the study of double-crystal OPOs are presented in Ref. [25].

Figure 4a presents the experimental tuning characteristic of OPO2 using two nonlinear HGS crystals. Two tuning curves correspond to two crystals HGS1 and HGS2. When the HGS1 crystal (θ = 60°) is rotated by ± 15° from the middle (normal) position, we observed continuous tuning of the idler wavelength of the OPO2 radiation within the range 4.18–5.6 μm. For the HGS2 crystal (θ = 47°) the tuning was observed in the range 5.6–10.8 μm. As a result, the total range of continuous tuning of the idler wavelength of OPO2 appeared to be 4.18–10.8 μm, which corresponds to the frequency interval ~1466 cm^{-1}. The slope of the tuning characteristic for the HGS1 crystal at the wavelength 4.7 μm amounted to ~0.26 nm step^{-1} (~0.12 cm^{-1} step^{-1}), and for the crystal HGS2 at the wavelength 7.45 μm it was approximately

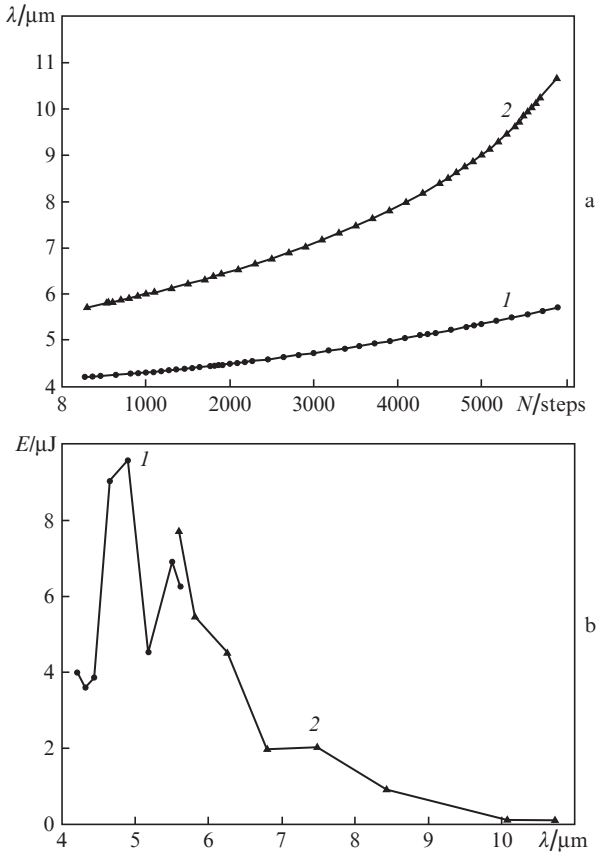

Figure 4. (a) Tuning characteristic of OPO2 (dependence of the wavelength on the position of the motorized rotary stage) and (b) dependence of the radiation pulse energy on the wavelength: (*1*) HGS1 crystal ($\theta = 60°$, $\varphi = 0$); (*2*) HGS2 crystal ($\theta = 47°$, $\varphi = 0$).

0.78 nm step^{-1} (~0.14 cm^{-1} step^{-1}). In the present work, the width of the OPO2 oscillation spectrum was not measured; however, for the HGS crystal under similar conditions in Ref. [23] it was ~2 cm^{-1}.

The dependence of the energy on the idler wavelength was investigated for OPO2. Figure 4b presents the dependences of the OPO2 radiation pulse energy on the wavelength. Two segments of experimental curves are shown, corresponding to the crystals HGS1 and HGS2. The OPO2 threshold at the wavelength 7.45 μm amounted to ~11 mJ cm^{-2}. As seen from Fig. 4b, when using the HGS1 crystal, the radiation pulse energy in the range 4.2–5.6 μm achieved ~9.6 μJ. The energy dip near 4.3 μm was observed due to the influence of light absorption by the atmospheric CO_2, as well as to the intrinsic absorption band of the HGS orange phase [21] itself. For the HGS2 crystal, the maximal energy of pulses (7.7 μJ) was observed near 5.7 μm, after which it monotonically decreased with increasing radiation wavelength. In the range 10–10.8 μm the radiation pulse energy amounted to ~1 μJ.

Figure 5 presents the calculated and experimental dependences of the phase matching angles in HGS crystals for the signal and idler wave for type II conversion (eo-e). The calculated dependences of the HGS phase matching angles were plotted using the improved-accuracy data from Ref. [24]. During our experiments, first, using the alignment laser, the positions corresponding to the normal angle of pump beam incidence were set for both crystals, and the wavelengths of the OPO2 radiation were measured. Then, using the tuning characteristic (see Fig. 4a) for HGS1 and HGS2, the external angles corresponding to the wavelengths measured in these positions were determined. The HGS phase matching angles were calculated using the improved-accuracy dispersion dependences, presented in Ref. [24]. In Fig. 5, the experimentally measured values of the phase matching angles for the crystals HGS1 and HGS2 are shown. One can see a practically complete coincidence of the calculated and the experimental dependences of the phase matching angles in the spectral ranges 1.17–1.41 μm (signal wave) and 4.18–10.8 μm (idler wave).

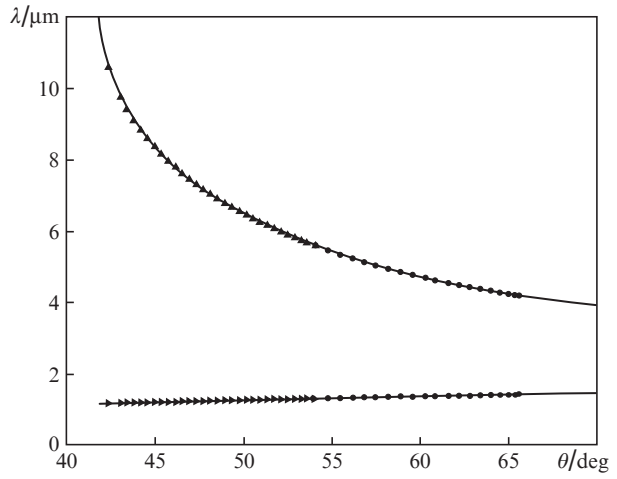

Figure 5. Calculated (solid lines) and experimental (points) dependences of the phase matching angles for HGS crystals (type II conversion, eo-e): the lower curve shows the signal wave, the upper curve – the idler wave, circles – HGS1 crystal ($\theta = 60°$, $\varphi = 0$), triangles – HGS2 crystal ($\theta = 47°$, $\varphi = 0$).

3.3. Recording the absorption spectra

The testing of the developed combined OPO was performed using a sealed-off gas-filled PA cell (see Fig. 1) by recording the absorption spectra of the gas components filling the cell. The PA cell is a nonresonance gas-filled photoacoustic detector. Its glass body had cylindrical shape with the diameter 12 mm and the length 12 mm. The ZnSe windows were glued to the faces of the cell, and a microphone connected with the internal volume was glued to the side wall of the cell. The cell was evacuated, tested for vacuum density and sealed-off. The composition of the gas mixture filling the PA cell (see Table 1) was chosen so that the absorption bands of different gas components of the mixture would not overlap, be well resolved, and uniformly fill the spectral range 2.5–11 μm. The information about the absorption spectra of gas admixtures was taken from the spectral database [8].

Table 1. Composition of the gas mixture filling the PA cell.

Gas admixture	Content (%)	Position of characteristic absorption peaks/μm [8]
Methane	10	3.32, 7.66
Nitrous oxide	5	2.87, 3.88, 4.47, 7.67, 16.9
Acetone	6	3.37, 5.75, 7.30, 8.22
Tetrafluoromethane	0.25	7.83
Sulphur hexafluoride	0.25	10.55
Nitrogen	78.5	–

Figure 6 presents the experimental spectrum of the gas mixture in the PA cell, obtained under the continuous tuning of the combined OPO wavelength within the range 2.5–10.8 μm. In this experimental record, one can select a few separate characteristic peaks of absorption (marked by figures 1–5) using which one can test the tuning characteristics of OPO1 and OPO2. They are as follows: 3.32 μm, the absorption peak of CH_4 (1); 4.47 μm, the absorption peak of N_2O (2); 5.75 μm, the absorption peak of acetone (3); 7.83 μm, the absorption peak of CF_4 (4); and 10.55 μm, the absorption peak of SF_6 (5).

Note that the range of OPO1 tuning (2.5–4.5 μm) contains peak 1 (methane) and weak bands of N_2O absorption, located around it. In the tuning range of HGS1 crystal of OPO2 (4.2–5.6 μm) there is strong peak 2 (N_2O). Absorption peaks 3 (acetone), 4 (CF_4), and 5 (SF_6) lie in the tuning range of the HGS2 crystal of OPO2 (5.6–10.8 μm).

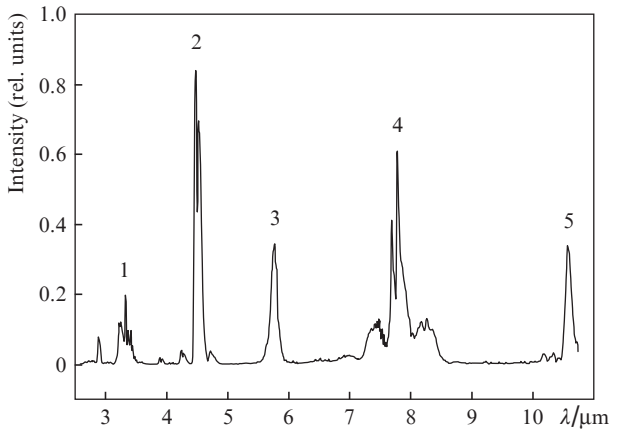

Figure 6. Absorption spectrum of the gas mixture in the range 2.5–10.8 μm, recorded using the combined OPO and the sealed-off gas-filled PA cell.

We propose to perform the automated testing of the combined OPO radiation wavelength calibration using the gas-filled sealed-off PA cell by recording the absorption spectrum of the gas mixture and comparing the positions of the characteristic absorption peaks in the current and reference spectrograms (the latter being stored in the computer memory).

4. Conclusions

We present the results of the development and testing of a combined OPO with continuous tuning of the radiation wavelength in the spectral range 2.5–10.8 μm (the frequency interval ~3074 cm^{-1}). The combined OPO comprises two separate OPO based on the 'fan-out' MgO:PPLN structure and the nonlinear HGS crystals, tunable in different spectral ranges, pumped with the radiation of a single Nd:YLF laser (λ = 1.053 μm).

OPO1 based on the 'fan-out' MgO:PPLN structure provided the continuous tuning of the idler wavelength within the range 2.5–4.5 μm (the frequency interval ~1777 cm^{-1}). The range of continuous tuning of OPO2 based on nonlinear HGS crystals amounted to 4.18–10.8 μm (the frequency interval ~1466 cm^{-1}). To reduce the required angular rotation of the nonlinear crystals in OPO2, we propose to use two nonlinear crystals cut at different angles θ instead of one crystal. In the spectral region 4.18–10.8 μm the phase matching angles in HGS crystals were experimentally determined for type II conversion, which practically coincided with the ones calculated in Ref. [24].

We propose to use a sealed-off gas-filled PA cell for testing the calibration of the combined OPO radiation wavelength by the position of characteristic absorption peaks of certain gas admixtures. The experimental absorption spectrum of the gas mixture in the range 2.5–10.8 μm is presented.

Acknowledgements. The authors express their gratitude to V.V. Badikov (Kuban State University) and V.Ya. Shchur (Ural Federal University) for placing nonlinear crystals and structures at our disposal, as well as for useful discussions and recommendations.

The work was carried out within the frameworks of the State Contract (No. 16.522.11.2001) of the Federal Programme 'Research and Development in Priority Areas for S&T Development in Russia for 2007–2013'.

References

1. Hinkley E.D. (Ed.) *Laser Monitoring of the Atmosphere* (Berlin: Springer-Verlag, 1976; Moscow: Mir, 1979).
2. Harren F.J.M., Bijnen F.G.C., Reuss J., Voesenek L.A.C.J, Blom C.W.P.M. *Appl. Phys. B*, **50**, 137 (1990).
3. Fink T., Buscher S., Gabler R., Yu Q., Dax A., Urban W. *Rev. Sci. Instrum.*, **67**, 4000 (1996).
4. Miklos A., Hess P., Bozoki Z. *Rev. Sci. Instrum.*, **72**, 1937 (2001).
5. Ponomarev Yu.N., Ageev B.G., Zigrist M.V., Kapitanov V.A., Courtois D., Nikiforova O.Yu. *Lazernaya optiko-akusticheskaya spektroskopiya mezhmolekulyarnykh vzaimodeystviy v gazakh (Laser Photoacoustic Spectroscopy of Intermolecular Interaction In Gases)* (Tomsk: MGP 'RASKO', 2000).
6. Karapuzikov A.I., Sherstov I.V., Ageev B.G., Kapitanov V.A., Ponomarev Yu.N. *Opt. Atmos. Okeana*, **20**, 453 (2007).
7. Stepanov E.V. *Trudy IOF RAN*, **61**, 5 (2005).
8. *NIST Standard Reference Database*: http://webbook.nist.gov/chemistry/.
9. Petrov V. *Progr. Quantum Electron.*, **42**, 1 (2015).
10. Angelmahr M., Miklos A., Hess P. *Appl. Phys. B*, **85**, 285 (2006).
11. Persijn S., Harren F., van der Veen A. *Appl. Phys. B*, **100**, 383 (2010).
12. Myers L.E., Eckardt R.C., Fejer M.M., Byer R.L., Bosenberg W.R., Pierce J.W. *J. Opt. Soc. Am. B*, **12**, 2102 (1995).
13. Powers P.E., Kulp T.J., Bisson S.E. *Opt. Lett.*, **23**, 159 (1998).
14. Adler F., Cossel K.C., Thorpe M.J., Hartl I., Ferman M.E., Ye J. *Opt. Lett.*, **34**, 1330 (2009).
15. Kolker D.B., Boyko A.A., Dukhovnikova N.Yu., Zenov K.G., Sherstov I.V., Starikova M.K., Miroshnichenko I.B., Miroshnichenko M.B., Kashtanov D.A., Kuznetsova I.B., Shtyrov M.Yu., Karapuzikov A.I., Karapuzikov A.A., Lokonov V.N., Zachariadis S. *Prib. Tekh. Eksp.*, **1**, 85 (2014) [*Instrum. Exp. Tech.*, **57** (1), 50 (2014)].
16. Vodopyanov K.L., Maffetone J.P., Zwieback I., Ruderman W. *Appl. Phys. Lett.*, **75**, 1204 (1999).
17. Vodopyanov K.L., Ganikhanov F., Maffetone J.P., Zwieback I., Ruderman W. *Opt. Lett.*, **25**, 841 (2000).
18. Badikov V.V., Don A.K., Mitin K.V., Seregin A.M., Sinaiskii V.V., Shchebetova N.I., Shchetinkina T.A. *Kvantovaya Elektron.*, **37**, 363 (2007) [*Quantum Electron.*, **37**, 363 (2007)].
19. Esteban-Martin A., Marchev G., Badikov V., Panyutin V., Petrov V., Shevyrdyaeva G., Badikov D., Starikova M., Sheina S., Fintisova A., Tyazhev A. *Laser Photon. Rev.*, **7**, L89 (2013).
20. Tyazhev A., Kolker D., Marchev G., Badikov V., Badikov D., Shevyrdyaeva G., Panyutin V., Petrov V. *Opt. Lett.*, **37**, 4146 (2012).
21. Badikov V.V., Kuzmin N.V., Laptev V.B., Malinovskii A.L., Mitin K.V., Nazarov G.S., Ryabov E.A., Seregin A.M., Shchebetova N.I. *Kvantvaya Elektron.*, **34**, 451 (2004) [*Quantum Electron.*, **34**, 451 (2004)].

22. Karapuzikov A.A., Sherstov I.V., Kolker D.B., Karapuzikov A.I., Kistenev Yu.V., Kuzmin D.A., Shtyrov M.Yu., Dukhovnikova N.Yu., Zenov K.G., Boyko A.A., Starikova M.K., Tikhonyuk I.I., Miroshnichenko I.B., Miroshnichenko M.B., Myakishev Yu.B., Lokonov V.N. *Phys. Wave Phenomena*, **22**, 189 (2014).
23. Tyazhev A., Marchev G., Badikov V., Esteban-Martin A., Badikov D., Panyutin V., Shevyrdyaeva G., Sheina S., Fintisova A., Petrov V., in *CLEO: Science and Innovations 2013*, *Tech. Dig*. (San Jose, Cal., 9–14 June 2013).
24. Kato K., Petrov V., Umemura N. *Appl. Opt.*, **55**, 3145 (2016).
25. Kostyukova N.Yu., Kolker D.B., Zenov K.G., Boyko A.A., Starikova M.K., Sherstov I.V., Karapuzikov A.A. *Laser Phys. Lett.*, **12**, 095401 (2015).